Spreading of a macroscopic lattice gas

S. F. Burlatsky,[1,2,*] J. G. Berberian,[2] J. Shore,[2] and W. P. Reinhardt[1]
[1]*Department of Chemistry, 351700, University of Washington, Seattle, Washington 98195-1700*
[2]*Department of Physics, Saint Joseph's University, 5600 City Avenue, Philadelphia, Pennsylvania 19131-1395*
(Received 5 January 1996)

We present a simple mechanical model for dynamic wetting phenomena. Metallic balls spread along a periodically corrugated surface simulating molecules of liquid advancing along a solid substrate. A vertical stack of balls mimics a liquid droplet. Stochastic motion of the balls, driven by mechanical vibration of the corrugated surface, induces diffusional motion. Simple theoretical estimates are introduced and agree with the results of the analog experiments, with numerical simulation, and with experimental data for microscopic spreading dynamics. [S1063-651X(96)04108-6]

PACS number(s): 03.40.Gc

I. INTRODUCTION

Because of its practical applications in areas such as coating, lubrication, and adhesion, the old field of wetting phenomena has recently attracted renewed interest [1–8]. Microdroplets that spontaneously spread along a solid surface have a time-dependent shape that results from the balance between liquid-solid interactions and friction processes [6]. Thus wetting mechanisms are intimately connected with friction on a molecular level [6,9,10] which is also important in the understanding of such practical problems as friction between two solid surfaces separated by a thin liquid layer [2] and dynamics of long polymer chains in random media [11].

A salient feature of macroscopic spreading is that it is often preceded by a microscopically thin film: a precursor. The precursor film thickness may vary from molecular size (one or sometimes several monolayers) to a few hundreds of angstroms [12]. For nonvolatile liquids, well below their critical temperature, thickness profiles with distinct successive molecular layers (terraces) have been observed [13,14]. Ellipsometric measurements, carried out on different substrates and also for various kinds of simple liquids, as well as polymeric and surfactant melts, have reached a surprising conclusion: the linear size R of the precursor obeys a universal law [13,15]

$$R \propto \sqrt{t}, \tag{1}$$

t being the time. The same law holds also for capillary rise, in which a vertical wall is put into a contact with a bath of liquid. Here a film of microscopic thickness grows from the macroscopic liquid meniscus and creeps upward along the wall. In this case, the height of the film obeys the $\sqrt{t}$ law within an extended time domain [16,17], until it gets truncated, at very high altitudes, by gravity. A diffusionlike coefficient D_1 can be formally defined as a prefactor in Eq. (1), which is found to scale as the inverse of the bulk viscosity. Such a formal fitting does not, however, immediately imply an understanding or even a model of the microscopic dynamics responsible for the simple power law [7].

Theoretical understanding of precursor dynamics has followed from two major conceptualizations: the hydrodynamic approach (HA) [18] and the solid on solid model (SOSM) [19], which is based on Langevin equations for layers in the drop. Both approaches qualitatively describe the formation of layered structures. The HA correctly describes long-term kinetics of terraced spreading in two-dimensional (2D) systems with cylindrical symmetry; however, the SOSM predicts $R \propto t$ rather than $\sqrt{t}$. In both models the layers are considered as being incompressible continua. Neither model assumes nor implies a microscopic model of the dynamics. An analogy with the analysis of macroscopically thin layers [8] and Ising-like models [3], as well as the diffusionlike structure of Eq. (1), suggests that diffusion inside the precursor layer plays an essential role for spreading dynamics. However, consideration of the motion of a precursor edge (PE) as a simple biased random walk is incorrect [8]. In the presence of an external force (capillary force that pulls the precursor out of the drop [7]), the mean displacement of a biased random walker (at the PE) is proportional to time in violation of Eq. (1), as is the prediction for the dynamics of the first layer in the SOSM [20]. In the absence of external forces the square root of the mean-square displacement would exhibit the behavior of Eq. (1). However, the mean PE displacement would be zero, contrary to wetting experiments, which indicate [7] a continuous directed displacement of the PE with relatively small fluctuations. This differs strongly from the fluctuation induced motion of a nonbiased random walker, where the fluctuations are of the same order as the typical displacement.

In [20,21] it was shown that the mean displacement of a random walker that is biased by a uniform external force and additionally experiences excluded volume repulsion exerted by an ensemble of other, nonbiased, diffusing hard-core particles grows in proportion to $\sqrt{t}$, instead of the linear in time growth expected for similar systems without the hard-core repulsion. We also have shown in this model that excluded volume effects imply an effective *frictional* force imposed on the motion of an individual particle in the hydrodynamic description.

*Permanent address: Institute of Chemical Physics, Russian Academy of Sciences, Moscow 117977, Russia. Electronic address: sfburlat@ringa.chem.washington.edu; sfburlat@sjuphil.sju.edu.

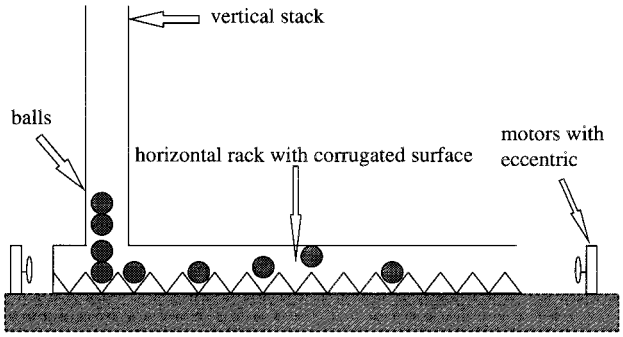

FIG. 1. Sketch of experimental setup.

The goal of the present work is to investigate a simple macroscopic spreading process with excluded volume. We consider the spreading of metallic balls, with and without magnetic interactions between the balls, and find that the spreading of balls in one dimension belongs to the same universality class as spreading of microscopic particles of liquids, i.e., is governed by Eq. (1). We present experimental results for the spreading of macroscopic balls, which emerge from a reservoir (vertical stack) and spread onto a horizontal vibrating rack; see Fig. 1. The surface of the rack is uniformly corrugated to prevent rolling or ballistic motion of the balls. Constraints enforce zero or unit occupancy of corrugated sites, creating a lattice system. Weak random driving leads to a *lattice-gas*-type behavior of the balls: random jumps of length ± 1 constrained by the excluded volume effect. We find that this analog model yields the $\sqrt{t}$ law for the total number of balls that emerge from the reservoir, for the average displacement of balls from the reservoir origin, and for the displacement of the rightmost ball. We also present analytical estimates and numerical simulations, which are in good agreement with experimental data. The results suggest that, as far as the time dependence is concerned, the $\sqrt{t}$ law is essentially independent of the nature of the interactions between the substrate and the spreading substance, long-range interactions between the particles themselves, as well as of the geometry and of the size of spreading particles. The prefactors in the square-root law, of course, do depend on the system's parameters and all details of the microscopic interactions.

The organization of the paper is as follows. In the Secs. II A and II B we describe the experimental setup and numerical algorithm, respectively. In Sec. III we present simple analytical results for our model: basic equations in Sec. III A; results for the flux of balls from the reservoir and averaged displacement of spreading balls in Sec. III B; results for the displacement of the rightmost ball, which determines the size of the spreading layer, in Sec. III C; and separate results for the steady regime that starts after the first ball falls out of the rack in Sec. III D. In Sec. IV we present experimental and numerical results, which are briefly summarized in Sec. V.

II. EXPERIMENTAL SETUP AND NUMERICAL PROCEDURE

A. Experiment

A schematic diagram of the experimental setup appears in Fig. 1. A corrugated (notched) horizontal rack is confined inside a rectangular tube, which prevents balls from passing one another or jumping off the track. A vertical stack is placed at the left end of the rack (at the origin) and metallic balls (balls) are fed through this stack, maintaining unit concentration of ''particles'' at the origin. The balls are allowed to move to the right of the origin only. The entire system is driven with motors placed on each end of the rack. The flywheel on each motor is eccentric to provide ''chaotic'' oscillations, which are experimentally shown (see below) to give rise to diffusional motion of the balls. A particular number of balls n ($n=4$ or 8) is placed in the vertical stack and then the oscillations are started. The time for the balls to leave the stack is measured and recorded along with the displacement of the horizontal balls. After this, n more balls are added to the stack and the procedure is repeated with the first n balls left at their respective place on the horizontal rack. The process is repeated until the rightmost ball reaches the right end of the rack. Results presented are averaged with respect to four independent trials. In a separate set of experiments the number of balls that emerge from the vertical stack as a function of time after the rightmost ball reached the right end of the rack and escape from the rack was measured. This is the spreading rate for a ''full'' horizontal rack. We used two kinds of balls: magnetic and nonmagnetic.

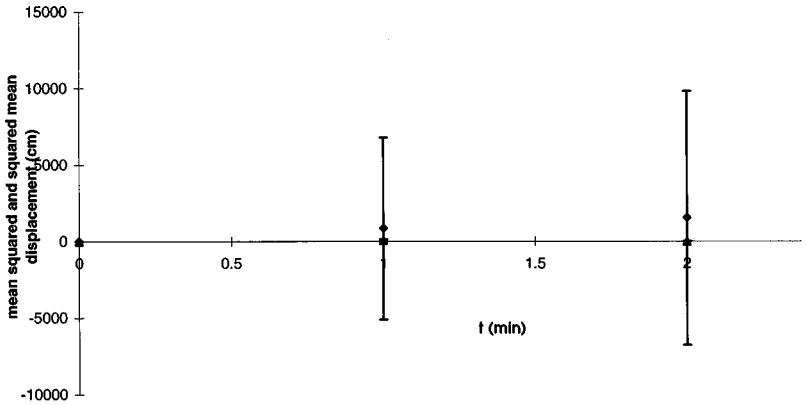

FIG. 2. Mean-square (diamonds) and squared mean (triangles) diplacement of a single ball vs time, averaged over 30 trials.

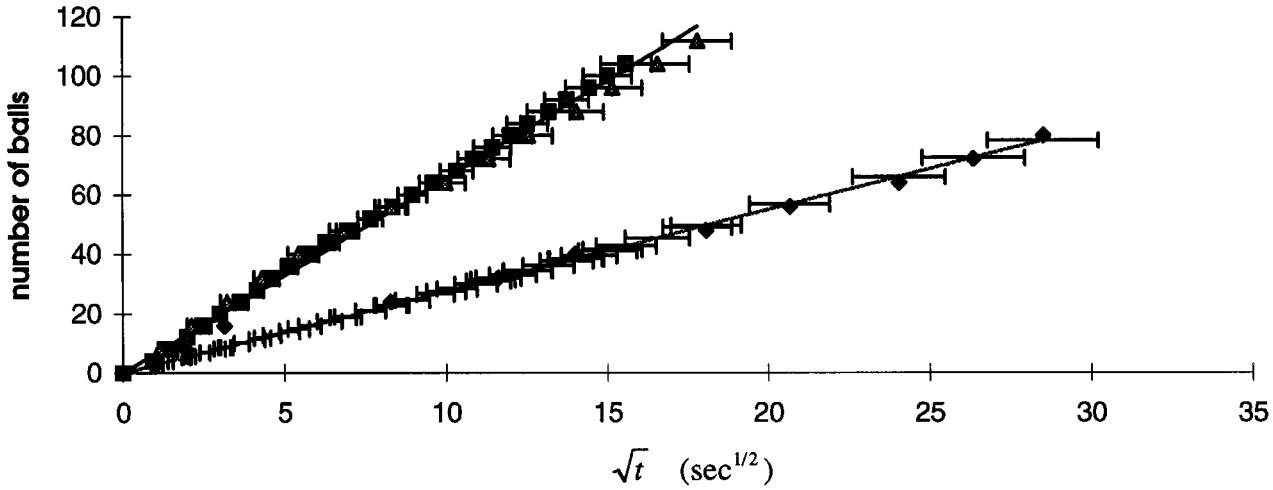

FIG. 3. Experimental dependence of the mean number of balls on a square root of time. Triangles, nonmagnetic balls, $n=8$; squares, nonmagnetic balls, $n=4$; diamonds, magnetic balls; solid lines, linear regression.

The experiment was designed to mimic the spreading of liquids: the vertical stack imitates a liquid drop, which acts as a reservoir providing particles for the precursor and keeps constant concentration at the drop-precursor boundary; the horizontal rack mimics a solid surface. Since the gravitational energy of balls on the rack is proportional to the height, the shape of the surface of the rack emulates the profile of the potential of liquid-substrate interactions with local potential minima, which prevent particles from long-range (on length scales larger than the mean distance between two neighboring particles) ballistic or rolling motion. Oscillations of the horizontal rack mimic thermal excitations of the surface of a solid substrate and generate random jumps of balls along the rack. The number n determines the gravitation-induced pressure in the vertical stack. Two sets of experiments, with $n=4$ and 8, were carried out in order to make sure that in a given range of n values the pressure is not important; see Sec. IV. The total number of balls on the horizontal stack $M(t)$ is an analog of the precursor mass and the displacement of the rightmost ball is an analog of the precursor radius $R(t)$. The magnetic mutual ball to ball attraction serves to mimic the particle-particle attraction in a precursor film and in a liquid drop.

To test the assumption that the eccentric oscillations generate diffusive motion of a single ball, Fig. 2 shows the mean-square displacement and the squared mean displacement of a single ball initially placed on the horizontal rack halfway between the origin and rightmost end. The observed linear dependence of the mean-square displacement on time agrees with the well-known result of conventional single-particle random-walk theory. The observed rms dispersion from the mean is also in approximate agreement with the prediction of simple estimates presented in the Appendix. However, the absolute values of dispersion is approximately 1.5 times greater than the theoretical value. These experimental results indicate that the jumps of a single ball are, to a good approximation, random and independent events caused by the vibrational driving of the system.

B. Numerical simulations

In numerical simulations, we modeled random jumps of particles on a 1D lattice with unit steps. For each time, each particle, except the particle in the site 0, chooses randomly a direction: to the right or to the left with equal probabilities. If the corresponding neighboring site is occupied, the move is rejected and the particle stays at the original position; if the site is vacant, the particle jumps to it. The origin (site 0) is always occupied; a new particle is automatically added to the site 1 when it becomes vacant. To simulate an analog of the magnetic interaction in the simplest manner, the jump rates of particles that had a nearest neighbor from one side to the vacant site on the other side was reduced by the factor $2(1-p)$, where p determines the ''strength of the interaction,'' $p=0.5$ corresponds to the absence of the interactions, and $p=1$ corresponds to infinitely strong attraction. At an initial time, two particles are placed into the system: the first particle at $i=0$ and the second particle at $i=1$. The mean displacement of balls was measured, as was the number of balls, as a function of time up to 100 active balls on the rack. Results were averaged with respect to 40 independent trials for each $p=0.5,0.6,0.7,0.8$.

III. SIMPLE ANALYTICAL ESTIMATES

A. Diffusion equation and boundary conditions

In order to obtain a simple analytical estimate for the dynamics of the processes we neglect mutual magnetic attraction (this is the same as neglecting surface tension for microscopic spreading phenomena) and decouple many particle probabilities. This leads to the following equations for mean concentrations in a 1D lattice with unit step (horizontal rack):

$$\begin{aligned}\frac{\partial C_v(i,t)}{\partial t}=\frac{\omega}{2}\{&C_v(i+1,t)[1-C_v(i,t)]\\&+C_v(i-1,t)[1-C_v(i,t)]\\&-C_v(i,t)[1-C_v(i-1,t)]\\&-C_v(i,t)[1-C_v(i+1,t)]\},\end{aligned}\tag{2}$$

where ω is frequency of jumps, which is connected to the diffusion coefficient $D=\omega l^2/2$, with l the jump length,

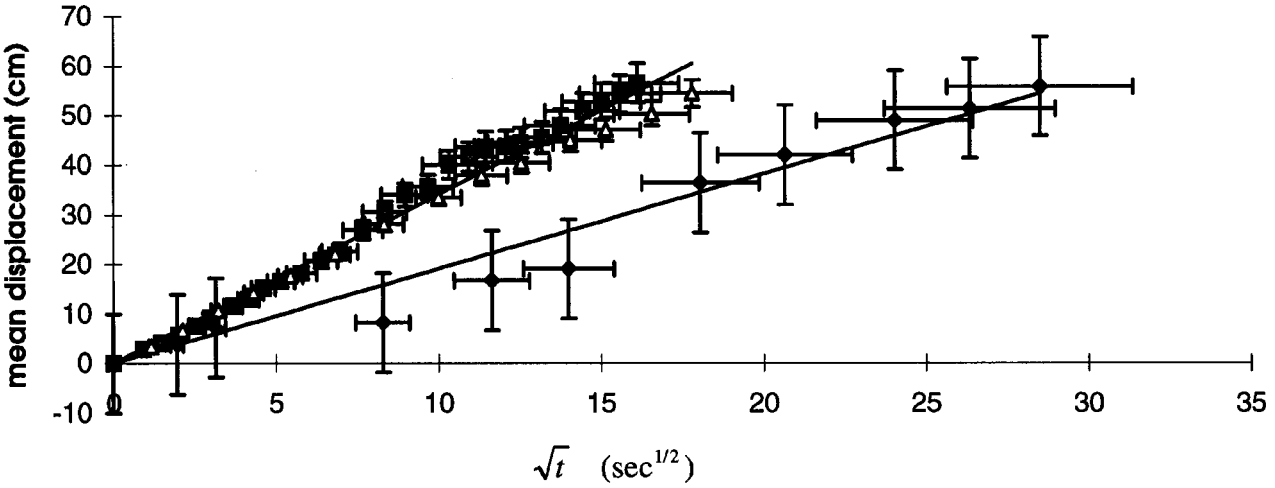

FIG. 4. Mean displacement of the rightmost ball vs the square root of time. Triangles, experimental data for nonmagnetic balls, $n=8$; squares, experimental data for nonmagnetic balls, $n=4$; diamonds, experimental data for magnetic balls; solid lines, linear regression.

$C_v(i,t)$ is concentration of vacancies (empty slots on the horizontal rack) at the slot i at time t, and $C_v(i,t)=1-C_b(i,t)$, with $C_b(i,t)$ is the probability to find a ball (ball) at slot i at time t. The first term on the right-hand side of Eq. (2) determines the rate of jumps of vacancies from the site $i+1$ to the site i. It is proportional to the concentration of vacancies at the site $i+1$ multiplied by the concentrations of particles at the site i since only vacancy-particle exchanges are allowed. The other terms determine the rate of jumps $i-1\rightarrow i$, $i\rightarrow i-1$, and $i\rightarrow i-1$ in a similar way.

In the approximate Eq. (2), nonlinear terms cancel since the forbidden particle-particle and vacancy-vacancy exchanges do not alter the local mean concentrations. When i and t are large, $i\gg 1$ and $\omega t\gg 1$, it leads to the diffusion equation

$$\frac{\partial C_v(i,t)}{\partial t}=\frac{\omega}{2}\Delta C_v(i,t), \tag{3}$$

where Δ is Laplace operator with respect to the variable i. At $t=0$ and $i>0$, there is no ''liquid'' on the solid surface (no balls on the horizontal rack). Therefore, the initial concentration of vacancies is equal to unity

$$C_v(i,t)|_{t=0}=1; \tag{4}$$

all sites are empty. When i is large the concentration of vacancies is equal to unity because the balls have not had enough time to reach this area,

$$\lim_{i\rightarrow\infty} C_v(i,t)=1. \tag{5}$$

There are no vacancies at the boundary $i=0$ because the reservoir of balls places a ball in the vacancy instantly,

$$C_v(i,t)|_{i=0}=0. \tag{6}$$

Note that, in spite of the fact that Eq. (3) apparently does not reflect the excluded volume interaction, the boundary condition Eq. (4) states that the ball from the vertical stack can move down to the horizontal rack if and only if the vacancy comes to the point $i=0$. When the ball falls down from the stack it eliminates the vacancy at $t=0$. The relaxation time for the vacancy concentration in the horizontal stack is determined by the diffusion of a vacancy through the array of balls in the horizontal stack: from the right end to the left end. Since the number of balls and the length of the array grow, the relaxation time increases, which slows down the dynamics and leads to the dependence presented by Eq. (1) instead of linear growth.

B. Flux from reservoir, number of balls, and averaged displacement

The solution of Eq. (3) in one dimension with the boundary conditions (4) and (5)

$$C_v(i,t)=1-\mathrm{erfc}\left(\frac{i}{2\sqrt{Dt}}\right) \tag{7}$$

leads to the result for the flux $P(t)$ at $i=0$,

$$P(t)=\frac{\omega}{2}\left.\frac{\partial C_v(i,t)}{\partial i}\right|_{i=0}=\sqrt{\frac{\omega}{2\pi t}}. \tag{8}$$

The number of particles on the rack is equal to

$$M(t)=\int_0^t P(\tau)d\tau=\sqrt{\frac{2\omega t}{\pi}}. \tag{9}$$

Writing down the equation similar to Eq. (2) for particles concentration, multiplying both sides of this equation by i, integrating from 0 to infinity, and taking into account the boundary conditions (6) and (5), we obtain, for the mean total displacement of all balls in the horizontal rack, $K(t)=\int_0^\infty iC_b(i,t)di$, measured in the jump length units l,

$$\frac{dK(t)}{dt}=\frac{1}{2}\omega. \tag{10}$$

Integrating Eq. (10) and taking into account the normalization

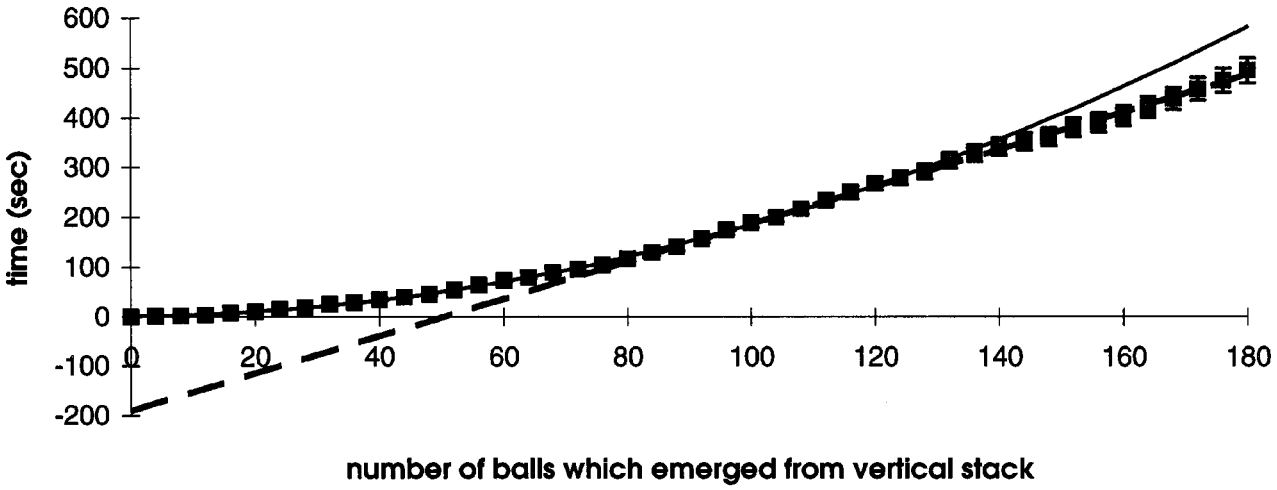

FIG. 5. Time vs the number of balls that emerged from the vertical stack. Squares, experimental data for nonmagnetic balls; solid line, theoretical dependence predicted by Eq. (9) for $t<t_0$; dashed line, theoretical curve, predicted by Eq. (16).

$$M(t)=\int_0^\infty C_b(i,t)di,$$

we obtain the averaged (over all balls) displacement for the balls in the horizontal rack $r(t)$,

$$r(t)\equiv\frac{K(t)}{M(t)}=\frac{1}{4}\sqrt{2\pi\omega t}. \tag{11}$$

The straightforward extension of the results (9) and (11) for the corresponding 2D system in the large-t limit leads to

$$P(t)|_{2D}=t\frac{2\pi a\omega}{2}\left.\frac{\partial C_v(i,t)}{\partial r}\right|_{i=0}\propto\frac{\pi\omega}{2\ln\left(\frac{Dt}{a^2}\right)} \tag{12}$$

and

$$M(t)|_{2D}\propto r(t)|_{2D}\propto\frac{\pi\omega t}{2\ln\left(\frac{Dt}{a^2}\right)}. \tag{13}$$

C. Displacement of the rightmost ball

One can show [22] that, apart from logarithmic corrections, which can occur in the long-time regime of spreading, the displacement of the rightmost ball on the horizontal rack [the length of the precursor $R(t)$] is proportional to the average displacement $R(t)\propto r(t)$, which leads to Eq. (1). Here we present a simple estimate for $R(t)$. The distribution of the displacement of the rightmost particle, for the ensemble of spreading hard-core particles, can be bounded by the maximum displacement of independent diffusing particles. The latter displacement has the distribution

$$P(R)=c(R,t)\exp\left(-\frac{1}{a}\int_0^R\ln[1-c(r,t)]dr\right), \tag{14}$$

where $c(R,t)=1-C_v(i,t)$, $C_v(i,t)$ being determined from Eq. (7). The first multiplier on the right-hand side of Eq. (11) is the probability to have a particular displacement R for a ball and the second term is a limiting continuum form for a probability to have smaller displacement for other balls. Averaging R with respect to the distribution Eq. (14) by means of the steepest decent method in the large-t limit, we obtain

$$\langle R\rangle=\sqrt{2Dt}\sqrt{\ln\left(\frac{16\,(Dt)^3}{\pi a^2}\right)}.$$

D. Steady regime

The regime of spreading changes after the first ball falls off the horizontal rack. The length of the array of balls does not grow anymore and the concentration of balls is determined by the steady-state solution of Eq. (3) with a new boundary condition on the right-hand side of the horizontal rack

$$C_v(i,t)|_{i=L}=1, \tag{15}$$

where L is the total number of slots on the horizontal rack. This boundary condition states that there are no balls out of the rack with the coordinates $i>K$. The solution of the steady state Eq. (3) leads to the constant flux of vacancies to the origin, which in turn leads to

$$M_1(t)=\frac{\omega}{2L}(t-t_0), \tag{16}$$

where M_1 is the number of balls that fall out of the rack and t_0 is the time when the first ball falls.

IV. EXPERIMENTAL AND NUMERICAL RESULTS

Figures 3 and 4 show the experimental results for the number of balls in the horizontal rack and the averaged displacement of the rightmost ball versus the square root of time for magnetic and nonmagnetic balls for $n=4,8$ and

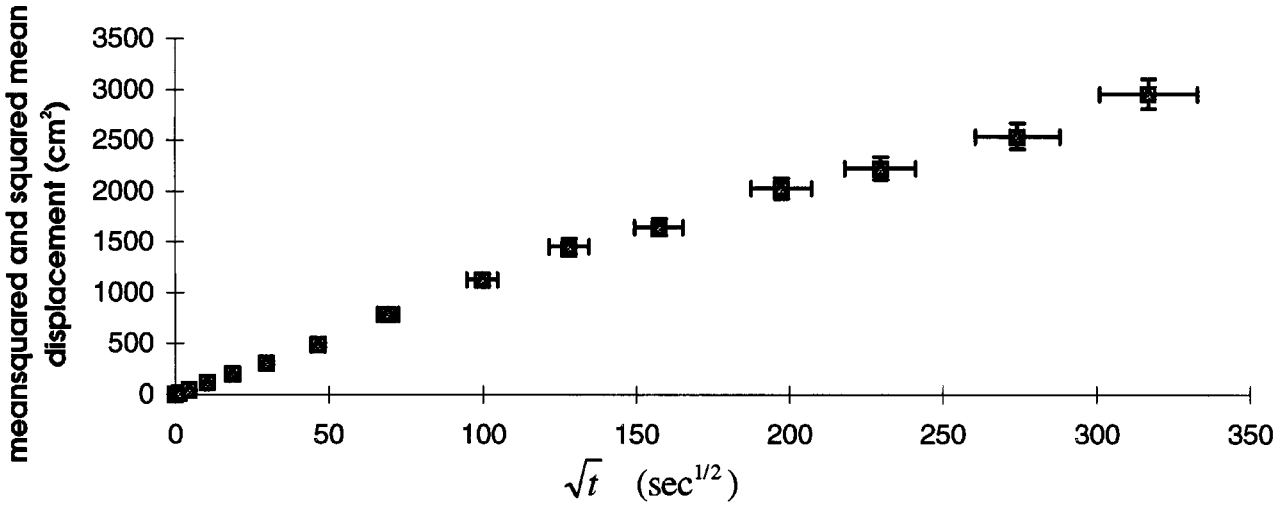

FIG. 6. Mean-square displacement (squares) and square of mean displacement (triangles) vs time for $n=8$ and nonmagnetic balls.

$t<t_0$. Figure 5 shows the time for a given number of balls to enter the horizontal rack from the stack. In this case the experiment was not interrupted at time $t=t_0$. Figure 6 presents the dependences of the mean-square displacement along with the squared mean displacement of the rightmost ball in the horizontal rack. Figures 7, 8, and 9 show the dependences of the mean number of balls in the horizontal rack, the mean displacement of balls on the horizontal rack, and the mean displacement of the rightmost ball versus the square root of time obtained in the numerical simulation for different values of the ''interaction parameter'' p, respectively.

The pronounced straight lines that are presented in Figs. 3, 4, and 6–8 are in good qualitative agreement with Eqs. (11), (9), and (1). However, the fluctuations in the dependence of the mean displacement on the square root of time are larger than fluctuations for the dependence of the total number of balls. The results for $n=4$ and 8 are essentially similar. It shows that the gravity-induced pressure in the reservoir does not play a significant role, which corresponds to the spreading of small droplets or vertical creep with relatively small precursor length where the gravitational forces are not important. In a test experiment with a larger number of balls $n\geqslant 40$, the large gravitational force pushed all balls from the vertical stack after the beginning of vibrations, overcoming the potential barriers produced by slots on the horizontal rack, i.e., large gravitational forces changed the nature of spreading.

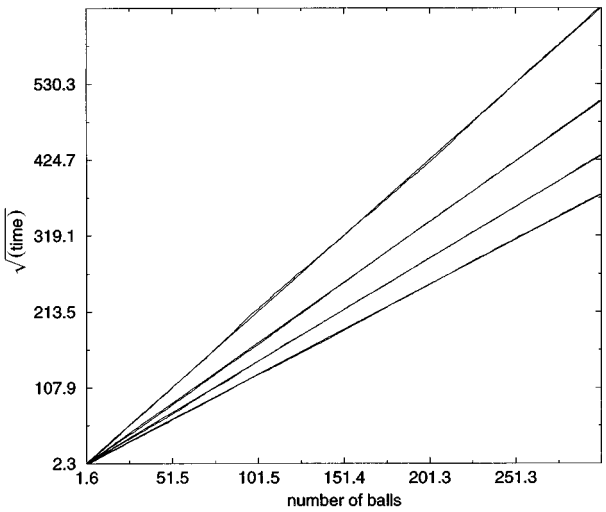

FIG. 7. Numerical data. The mean number of balls on the horizontal rack p grows from 0.5 to 0.8.

The theoretical values for the slopes of the linear dependences of the number of balls and of the mean displacement of balls in the precursor that are determined by Eqs. (9) and (11) for $\omega=1$, $\sqrt{2/\pi}\approx 0.798$ and $\sqrt{2\pi}/4\approx 0.6266$, are in excellent agreement with the corresponding values determined from the numerical experiment, 0.804 and 0.625. The magnetic interaction does not change the shape of the dependences but decreases the numerical prefactors and increases fluctuations. Introduction of the effective interaction in numerical simulations leads to similar effects. The numerical results for the dependences of the mean number of balls on the horizontal rack and of the mean displacement versus square root of time, presented in Figs. 7 and 8, exhibit a slowing down when the interaction parameter increases from 0.5 to 0.8. The fluctuations in the mean-square displacement also increase and the crossover period, which can be seen for small times in Fig. 8, becomes larger.

It is also instructive to compare the results presented in Fig. 2 for the moments of the displacement of the single ball on the horizontal rack with the results for the moment of the displacement of the rightmost ball of the array spreading along the rack, presented in Fig. 6. For a single ball the mean-square displacement is proportional to time, while the squared mean displacement is much smaller and irregular. In the limit of a large number of trials K, it should tend to zero as $1/\sqrt{K}$. On the contrary, the experimentally measured

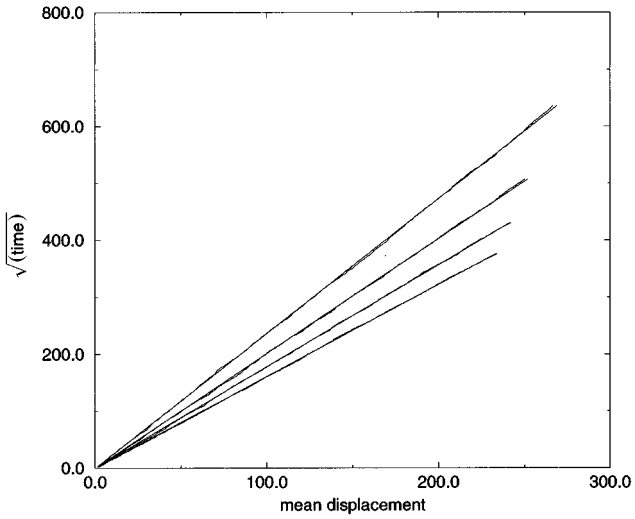

FIG. 8. Numerical data. The mean displacement averaged for all balls on the horizontal stack p grows from 0.5 to 0.8.

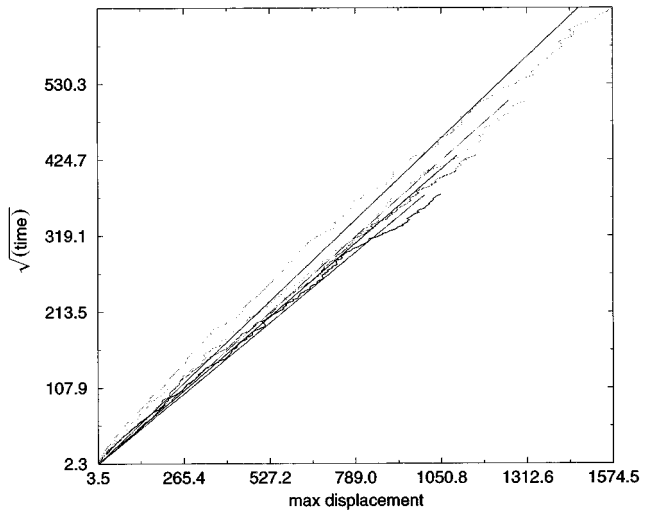

FIG. 9. Numerical data. The mean displacement of the rightmost ball along the horizontal stack p grows from 0.5 to 0.8.

mean-square displacement and squared mean displacement for the rightmost ball in the array are equal within the error of the experiment. This shows that, in spite of apparent scaling, the similarities of these two processes are of essentially different physical origin and behavior. The motion of a single ball is a fluctuation-induced process with zero mean, while the spreading is a driven diffusive process with small fluctuations.

The initial parabolic dependence presented in Fig. 5 for $t<t_0$ agrees with Eq. (9), while the linear dependence obtained for $t>t_0$ confirms Eq. (16). The numerical prefactors for these time dependences are not the subject of our present work; thus actual values of the vibrational frequencies and length scales are not important for our results. However, we can suggest some rough estimates, which produce reasonable numerical values. The effective experimental frequency of jumps $\omega\approx 32\ \mathrm{sec}^{-1}$ was roughly estimated from the data presented in Fig. 5 for the time $t>t_0$ (the liner regime) with the approximate values for the length of the rack ≈ 60 cm and $l\approx 1$ cm. It is in good agreement with the value $\omega\approx 36\ \mathrm{sec}^{-1}$, which was obtained by independent estimate from the region $t<t_0$ by means of Eq. (9). The slope for the experimental dependence of mean displacement versus the square root of time is also in good agreement with the theoretical estimate.

V. SUMMARY

We have calculated analytically, simulated numerically, and measured experimentally the mass and the size of a wetting layer for a simple mechanical system: metallic balls, which spread along a periodically corrugated surface, which mimics the wetting phenomena. The experimental results and numerical data are in excellent agreement with the theoretical predictions concerning the dependences that determine the dynamics of spreading of a lattice gas (balls) in our mechanical model [23]. These agree with Eq. (1), which empirically describes the dynamics of precursors in the spreading of actual liquid drops. The mechanical model may thus reflect the important features of this phenomenon, which lead to the universal spreading law Eq. (1). Analysis of the experimental results, simple analytical estimates, and numerical simulations provides an additional argument that the precursor kinetics is controlled by the diffusion of vacancies from the precursor's boundary to the liquid drop [1–3,6,22]. A theoretical model that directly explores the consequences of these ideas for a model of microscopic wetting is presented in a subsequent paper [22], which substantially extends the ideas of [24].

ACKNOWLEDGMENTS

The authors thank S. Granick, A.M. Cazabat, M. Robbins, M. Moreau, and G. Oshanin for helpful discussions. This work was supported in part by ONR Grant No. N00014-94-0647.

APPENDIX: DISPERSION OF MEAN-SQUARED DISPLACEMENT

Let us consider the dispersion for the average over K realizations squared displacement of a random walk containing N steps. What we measure is the mean-square displacement for an individual random walk

$$\langle R_i^2(N)\rangle=\left\langle\left(\sum_{j=1}^{N} s_i\right)^2\right\rangle=\sum_{j=1}^{N}\langle s_j^2\rangle,$$

where s_j is the step number j. $R_i^2(N)$ is the squared displacement of the random walk number i, $R_i^2(N)=(\Sigma_{j=1}^{N}s_i)^2$; the average of the squared displacement is

$$\frac{\sum_{j=1}^{K} R_i^2(N)}{K} = \frac{\sum_{j=1}^{K} \left(\sum_{j=1}^{N} s_i \right)^2}{K};$$

Δ and Δ^2 are defined as follows:

$$\Delta = \sqrt{\sum_{i=1}^{K} \left(R_i^2(N) - \frac{\sum_{i=1}^{K} R_i^2(N)}{K} \right)^2 \Big/ K};$$

and denoting $R_i^2(N) = X_i$,

$$\Delta^2 = \sum_{i=1}^{K} \left(X_i - \frac{\sum_{i=1}^{K} X_i}{K} \right)^2 \Big/ K = \sum_{i=1}^{K} (X_i)^2 - \sum_{i=1}^{K} \left(\frac{\sum_{i=1}^{K} X_i}{K} \right)^2 \Big/ K.$$

All $R_i(N)$ are independent random variables with zero mean and second moment equal to $N\sigma^2$. The Gaussian random variables $R_i^2(N)$ have a mean equal to $N\sigma^2$ and the second central moment equal to $3N^2\sigma^4$. For $K=30$, $\sqrt{30} \propto 5.4772$, $1/\sqrt{30} = 0.182\,57$, and $\Delta = \sqrt{3/\sqrt{30}} N\sigma^2 = 0.740\,08 N\sigma^2$.

[1] J. D. Coninck, N. Fraysse, M. Valignat, and A. Cazabat, Langmuir **9**, 1906 (1993).
[2] S. Granick, in *Fundamentals of Friction*, Vol. 220 of *NATO Advanced Study Institute, Series B: Physics*, edited by I. L. Singer and H. N. Pollock (Kluwer, Dordrecht, 1992).
[3] A. L. K. K. D. Abraham, Phys. Rev. E **51**, 51 (1995).
[4] K. Kaski, Europhys. News **26**, 23 (1995).
[5] J. A. Nieminen, D. B. Abraham, M. Karltunen, and K. Kaski, Phys. Rev. Lett. **69**, 124 (1992).
[6] P. de Gennes, Rev. Mod. Phys. **57**, 827 (1985).
[7] A. M. Cazabat, Contemp. Phys. **28**, 347 (1989).
[8] J. J. P. de Gennes, J. Phys (Paris) **47**, 121 (1986).
[9] R. Overney *et al.*, Phys. Rev. Lett. **72**, 3546 (1994).
[10] P. Tompson, G. Grest, and M. Robbins, Phys. Rev. Lett. **66**, 3448 (1992).
[11] S. Burlatsky and J. Deutch, Science **260**, 1782 (1993).
[12] W. B. Hardy, Philos. Mag. **38**, 49 (1919).
[13] F. Heslot, N. Fraysse, and A. Cazabat, Nature **338**, 640 (1989).
[14] M. Valignat, N. Fraysse, A. Cazabat, and F. Heslot, Langmuir **9**, 601 (1993).
[15] F. Tiberg and A. M. Cazabat, Europhys. Lett. **25**, 205 (1994).
[16] F. Heslot, A. M. Cazabat, and N. Fraysse, J. Phys. Condens. Matter **1**, 5793 (1989).
[17] A. M. Cazabat, N. Fraysse, and F. Heslot, Colloids Surf. **52**, 1 (1991).
[18] P. de Gennes and A. Cazabat, C. R. Acad. Sci. **310**, 1601 (1990).
[19] D. B. Abragam, P. Collet, J. D. Coninck, and F. Dunlop, Phys. Rev. Lett. **65**, 195 (1990).
[20] S. Burlatsky, G. Oshanin, A. Mogutov, and M. Moreau, Phys. Lett. A **166**, 230 (1992).
[21] S. Burlatsky, G. Oshanin, M. Moreau, and W. Reinhardt, Phys. Rev. E (to be published).
[22] S. Burlatsky, A. M. Cazabat, G. S. Oshanin, M. Moreau, and W. P. Reinhardt, Phys. Rev. E (to be published).
[23] Calculation of the numerical prefactors in some cases requires a more elaborate theory.
[24] S. F. Burlatsky, W. P. Reinhardt, G. S. Oshanin, and M. Moreau, Bull. APS **40**, 301 (1995).